Multimedia Tools and Applications (2020) 79:15513–15530
https://doi.org/10.1007/s11042-019-7459-x

Adaptive fuzzy hexagonal bilateral filter for brain MRI denoising

Kala R[1] · Deepa P[1]

Received: 30 September 2018 / Revised: 9 January 2019 / Accepted: 7 March 2019 /
Published online: 3 April 2019

Abstract
Magnetic resonance image (MRI) plays a crucial role in medical applications for visual analysis and processing. Rician noise which arises from the MRI during acquisition can affect the quality of the image. This crucial issue should be addressed by denoising method. The proposed adaptive rician noise removal based on the bilateral filter using fuzzy hexagonal membership function improves the denoising efficiency at various noise variances and preserves the fine structures and edges. The fuzzy weights were obtained with the local mean (μ_i) and global mean (μ_g) by constructing hexagonal membership function for local order filter and bilateral filter. Bilateral filter is used to preserve the edges by smoothening the noises in MRI image and local filter is used to preserve the edges and retrieve the structural information. Brain MRI images are restored by multiplying its corresponding fuzzy weight with the restored image of local order filter and bilateral filter. Experiments on synthetic and clinical Brain MRI data were done at different noise levels by the proposed method and the existing methods. The result shows that the proposed method restores the image in better visual quality and can be well utilized for the diagnostic purpose at both low and high densities of rician noise.

Keywords Magnetic resonance imaging · Rician noise · Fuzzy logic · Denoising · Membership function · Bilateral filtering

1 Introduction

Magnetic resonance imaging (MRI) is a significant powerful imaging techniques and effective diagnostic tool developed to analyze the anatomical and physiological information of internal

✉ Kala R
kalarajamani04@gmail.com

Deepa P
deepap05@gmail.com

[1] Department of Electronics and Communication Engineering, Government College of Technology, Coimbatore, Tamilnadu 641 013, India

body parts [38]. MRI images are affected by thermal noise during acquisition and decrease the quality of the acquired images [11, 16, 21, 26]. The restoration of noisy image without degrading the fine structural features has been a crucial issue in MRI analysis [10]. Need of noise reduction technique for medical image is a vital issue in medical field. Different kinds of noises like salt & pepper, speckle, gaussian, rician, rayleigh, gamma, uniform, poisson etc. are present in medical image [1, 2]. The most frequently occurring noise in MRI images is the rician noise. The complexity in restoring high resolution MRI increases due to rician noise. The low signal to noise ratio (SNR) creates random variation and the signals dependent on bias which reduces the brightness and contrast of the image [28, 29]. This work is to improve energy consumption, reliability and better lifetime. It provides the hybrid solution. The watermarking has to be done for the restoration for achievement of good quality in the images [4, 6, 22].

Many researchers developed diverse techniques to restore the MRI images affected by rician noise. The estimation of magnitude MRI from the degraded image has been proposed but limits to low noise variation [13]. Gaussian filters have been extensively used in MRI pre-processing during restoration, results in blurred edges at high-frequency signals [8]. Various edge-preserving methods have been projected for medical image denoising to overcome the blurring effects and they do not degrade the morphological edges during smoothing [17]. The anisotropic diffusion filters removes noise using gradient information at low noise level rather than high noise level [12]. Homogeneity mean difference (HMD) method is sensitive to noise and insensitive to contrast during image restoration [37]. In [23] noises in the brain images were detected and removed using directional filtering algorithm but it takes more complexity. Wavelet based bilateral filter with neigh shrink preserves the structural features, but the strong noisy pixels in homogeneous regions were not reduced [7]. MRI enhancement using genetic programming for rician noise removal preserves the structural details, but complexity increases in setting the parameters for genetic programming and requires more time to converge [20].

Rough set based bilateral filter approach derives pixel level edge map and class labels to achieve better restoration but the restoration potential needs to be improved [31]. Non-local means (NLM) algorithms were efficiently used in MRI denoising, but limited due to high computational complexity. The random sampling based NLM algorithm decreases the computational burden, but the restoration potential needs to be improved [15]. Linear minimum mean square error (LMMSE) filtering removes the rician noise with less restoration efficiency [36]. The choice of bilateral filter parameters affects the performance of denoising. In order to get the optimised parameters, genetic algorithms have been applied to the noisy images in searching regions of different window size and the efficiency of the filter mainly depends upon the optimal parameter selection [3]. Iterative bilateral filter improves the denoising efficiency, preserves the fine structures and reduces the bias due to rician noise but the complexity increases due to increase in number of iterations [32].

To overcome these challenges, machine learning techniques such as fuzzy logic based system are widely used for solving problems in different domain of engineering [5, 9] and in medical application it is based on image-based diagnosis, disease detection and disease prognosis to reduce the operator dependency and get better diagnostic accuracy [19]. Trapezoidal fuzzy based hybrid filter preserves edges but does not give a suitable degree of membership to the filters to restore the MR image [35]. In fuzzy similarity based NLM filter for rician noise removal, the structural information has not been retrieved properly from noisy image [34]. The adaptive hexagonal fuzzy hybrid filter for rician noise removal in MR images restores the image at low and high densities of rician noise [18]. However, the problem of

image restoration still remains open because it is an ill-posed inverse problem; it requires necessary information about the degraded image to reconstruct the original image. Therefore, the need for more effective methods keeps increasing. The proposed adaptive fuzzy hexagonal bilateral filter removes the rician noise by preserving the structural information. The proposed filter combines the median filter and bilateral filter adaptively by constructing the fuzzy hexagonal membership function using local and global statistical parameters.

The rest of the paper is organised as follows. Section 2 briefly discusses the proposed adaptive fuzzy hexagonal bilateral filter for brain MRI restoration. Section 3 provides the information on experimental setup. Section 4 discusses the analysis of the proposed adaptive fuzzy hexagonal bilateral filter effect for synthetic and clinical MRI data. Finally Section 5 concludes the paper.

2 Adaptive fuzzy hexagonal bilateral filter

The proposed adaptive fuzzy hexagonal bilateral filter along with local order filter removes the rician noise in MRI under low and high noise levels. The acquired MRI data are complex and represented in frequency domain as k-space [35]. The raw data has been corrupted by thermal noise during acquisition [36]. After inverse fourier transformation of the k-space data, the resultant data are complex and still corrupted by noise. The magnitude computation is a non-linear operation, changes to rician by realizing the probability distribution function (PDF) of noise in the image [35]. The PDF of MR signal (M) magnitude data is given as

$$p(M|A,\sigma) = \frac{M}{\sigma^2}\exp\left(-\frac{M^2+A^2}{2\sigma^2}\right)I_o\left(\frac{AM}{\sigma^2}\right)u(M) \tag{1}$$

where, A represents the amplitude of noise free signal, σ^2 refers to variance of white Gaussian noise, I_o denotes the modified Bessel Function in zero order and u (M) represents unit step Heaviside function that indicates the PDF of M is valid for non negative values of M [36].

The proposed adaptive fuzzy hexagonal bilateral filter removes the rician noise in MRI is shown in Fig. 1. The method is based on fuzzy logic that combines local order filter and bilateral filter to restore the MRI. The proposed method determines the statistical features such as local mean, global mean and standard deviation of the noisy image. The fuzzy weights are computed adaptively using hexagonal membership function at both low and high noise levels to restore the MR image as shown in Fig. 1 where $W_{bilateral}$ and W_{local} are the fuzzy weights for the noisy MRI image.

2.1 Statistical features

The statistical features such as standard deviation, local mean, and global mean are computed using (2) and (3) [35]. To differentiate background and foreground regions of the image, local mean (μ_i) of a local neighbourhood and global mean (μ_g) of a noisy image are considered to construct fuzzy membership function. In magnitude MR data the standard deviation of the rician noise is computed using (2)

$$\sigma_g = \sqrt{\frac{\mu_b}{2}} \tag{2}$$

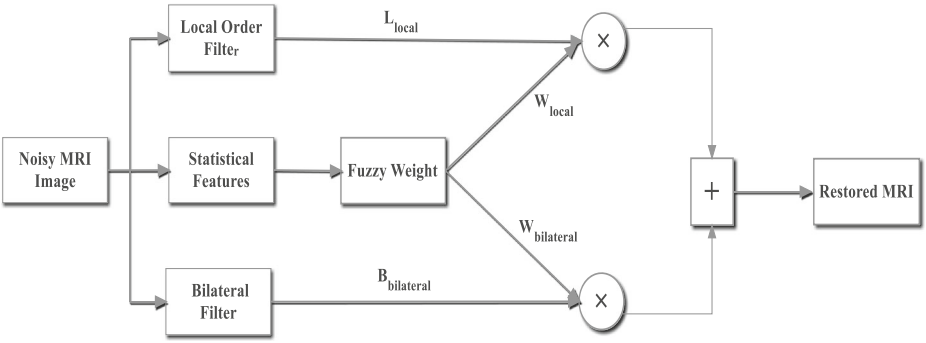

Fig. 1 Block diagram of the proposed adaptive fuzzy hexagonal bilateral filter

where μ_b is the mean value of the background region of MR image.

$$\mu_b = \frac{1}{m \times n} \sum_{i,j=1}^{m,n} f(i, j) \tag{3}$$

f(i, j) is the input MRI image of size m × n. Background is extracted using Otsu threshold method [35].

2.2 MRI denoising using local order and bilateral filter

The local order and bilateral filter are applied to the noisy MR image. The local order filter is the high pass filter works well at low level noise in MRI image by retaining the edges. The bilateral filter is a non linear filter, preserves the edges and removes the noise effectively. The local order and bilateral filter are applied along with the corresponding fuzzy weights determined by using hexagonal membership function suppress the rician noise.

2.2.1 Local order filter

The local order filter is used to remove the highly corrupted pixels. It uses the search window size $(2 \times M_{local} + 1)$ with a mask of size $(2 \times R_{local} + 1)$ to perform convolution over the complete noisy MR image. The M_{local} and R_{local} are set to one and compute the median value for each pixel in the image [35]. The restored image for local-order statistical filter is given by

$$L_{local} = \text{LocalFilter}\,(L, R_{local}) \tag{4}$$

where, L_{local} is the local order filter image of the noisy MR image L and R_{local} is the radius of squared neighbourhood pixel.

2.2.2 Bilateral filter

The bilateral filter uses the combination of the weight obtained in range filter and domain filter for removing the noise in MR image. The bilateral filter smoothens and preserves edges of the noisy MR image. The bilateral filter for image restoration is given in (5).

The weights of the domain and range filter are given in (6) & (7) respectively. The weight of the domain filter is computed as spatial distance between the pixels and the range filter is the intensity difference between the pixels.

$$B_{bilateral} = \frac{1}{w_p} \sum_{x \in \Omega} w_d \; w_r \; f(x) \tag{5}$$

where,

$$w_d = e^{-\frac{1}{2}\left(\frac{d(p-s)}{\sigma_d}\right)^2} \tag{6}$$

$$w_r = e^{-\frac{1}{2}\left(\frac{\delta(I_p - I_s)}{\sigma_r}\right)^2} \tag{7}$$

and

$$w_p = \sum_{x \in \Omega} w_d \; w_r$$

$f(x)$ is the input MR image, w_d, w_r and w_p are the weights of the domain filter, range filter and normalization parameter respectively. Ω is the neighbourhood of a centre pixel. σ_d and σ_r controls the decay of two weight factors, d (p-s) is the Euclidean distance between current pixel (p) and neighbour pixel (s), $\delta(I_p - I_s)$ is the difference between two intensity values [32].

2.3 Adaptive fuzzy hexagonal membership function

An adaptive fuzzy hexagonal membership function restores the noisy MRI using the statistical features. Membership function (MF) is a hexagonal curve that defines the mapping of each pixel in the input MR image to the corresponding membership value between 0 and 1 as given in (9). Fuzzy hexagonal membership function has been constructed adaptively by using statistical features for better restoration. The hexagonal MF shown in Fig. 2 has been denoted using (9).

$$f(x;a,b,c,d,e,f) = \begin{cases} 0 & for\ x < a \\ \frac{1}{2}\left(\frac{x-a}{b-a}\right) & for\ a \le x \le b \\ \frac{1}{2} + \frac{1}{2}\left(\frac{x-b}{c-b}\right) & for\ b \le x \le c \\ 1 & for\ c \le x \le d \\ 1 - \frac{1}{2}\left(\frac{x-d}{e-d}\right) & for\ d \le x \le e \\ \frac{1}{2}\left(\frac{f-x}{f-e}\right) & for\ e \le x \le f \\ 0 & for\ x > f \end{cases} \tag{9}$$

where x is the input value for the hexagonal function and a, b, c, d, e and f are scalar parameters, computed using (10).

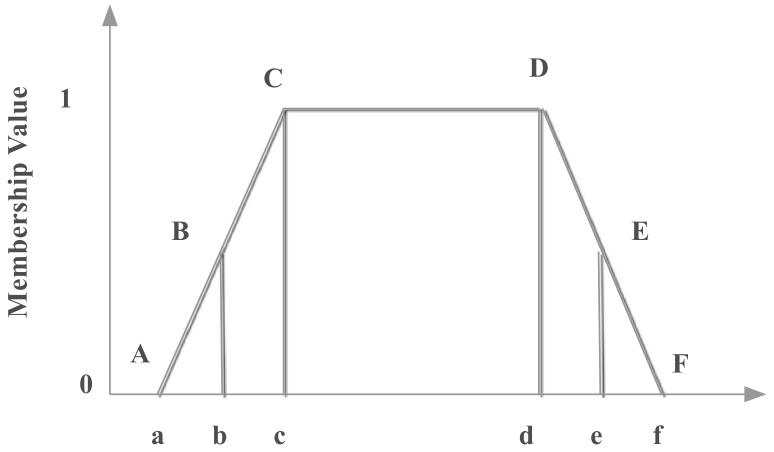

Fig. 2 Hexagonal Fuzzy Membership Function

$$\begin{aligned} a &= k_1 \times \min\left(\mu_{i,}\mu_g\right) \\ b &= k_2 \times \max\left(\mu_{i,}\mu_g\right) \\ c &= k_3 \times b \\ d &= k_4 \times c \\ e &= k_5 \times d \\ f &= k_6 \times e \end{aligned} \tag{10}$$

where k_1, k_2, k_3, k_4, k_5, and k_6 are adjusting parameters and it depends on noise level σ_g. μ_i is the mean of a local neighbourhood centred around a pixel i and μ_g is the mean of the complete image. The adjusting parameters k_1 and k_2 have been considered as given in (11) [35]. The k_3, k_4, k_5, and k_6 are obtained by conducting the experiment based on trial and error method.

$$\begin{aligned} k_1 &= 3.1 \times \sigma_g \\ k_2 &= 0.98 + 0.8 \times \sigma_g \\ k_3 &= 4.1 \\ k_4 &= 3.1 \\ k_5 &= 2.1 \\ k_6 &= 1.1 \end{aligned} \tag{11}$$

After the construction of fuzzy hexagonal membership function, weight of bilateral and local order are computed as given in (12),

$$\begin{aligned} W_{bilateral} &= f(\mu_i; a, b, c, d, e, f) \\ W_{local} &= 1 - W_{bilateral} \end{aligned} \tag{12}$$

where $W_{bilateral}$ and W_{local} are the near optimal contributions of bilateral and local filters respectively.

The restored image is obtained using (13),

$$f(x, y) = W_{bilateral} \times B_{bilateral} + W_{local} \times L_{local} \tag{13}$$

PSEUDOCODE

Input: Original MRI image with rician noise [f(i,j)]
Output: Restored MRI image [f(x,y)]

begin

// Statistical features
for every pixel in the noisy image
do
// find the mean of the local window (neighbourhood)
$\mu_i = E(W_i)$
end
for every pixel in the noisy image
do
// find the global mean of the image (complete image)
$\mu_g = E(W_g)$
end
// Estimate the rician noise from background of magnitude MRI image.
for every pixel in the noisy image
do

$$\sigma_g = \sqrt{\frac{\mu_b}{2}}$$

end

// Local order filter
for every pixel in the noisy image
do
sort values in the mask
pick the middle one in the sorted list
replace the pixel value with median one
L_{local} = *median filter*
end

// Bilateral filter
for every pixel in the noisy image
do
// find the weight of the range filter

$$w_r = e^{-\frac{1}{2}\left(\frac{\delta(I_p - I_s)}{\sigma_r}\right)^2}$$

// find the weight of the domain filter

$$w_d = e^{-\frac{1}{2}\left(\frac{d(p-s)}{\sigma_d}\right)^2}$$

// Bilateral filter output

$$B_{bilateral} = \frac{1}{w_p}\sum_{x\in\Omega} w_d\, w_r\, f(x)$$

end

// calculate the weights using fuzzy hexagonal membership function
for every pixel in the noisy image
do
$W_{\text{bilateral}} = f(x; a, b, c, d, e, f)$ *from Eq. (9)*
$W_{local} = 1 - W_{\text{bilateral}}$
// compute restored image
$f(x, y) = W_{\text{bilateral}} \times B_{\text{bilateral}} + W_{\text{local}} \times L_{\text{local}}$
end
end

3 Experimental setup

Quantitative and Qualitative analysis are performed for the synthetic and clinical MRI using the proposed method and existing methods. Quantitative analysis is performed by the performance metrics peak signal to noise ratio (PSNR), root mean squared error (RMSE) and the structural similarity index measure (SSIM). Qualitative analysis is done by the visual assessment of the restored MRI image.

3.1 Synthetic MRI data set

The synthetic data sets of the normal brain MR images are taken from the BrainWeb for analysis. The three co-registered modalities named: T1- weighted, T2-weighted, and PD-weighted are considered with the size 181× 128× 181. The voxel resolution of the datasets is $1mm^3$. Different slices are taken for the analysis.

3.2 Clinical MRI data set

The clinical MR data sets of the brain MR images are obtained for analysis from the Medall Diagnostics at Tirunelveli for co-registered three modalities: T1-weighted, T2-weighted, and PD-weighted. Conventional T1, T2, and PD weighted MR image are measured with angles 700, 2200 and 2200 respectively, of the same spin echo sequence are considered for analysis with 30 number of 2-D slices in each volume. The public MR data sets of the brain MR images [14] for T1-weighted, T2-weighted, and PD-weighted have been analyzed for different slices.

3.3 Performance metric and parameter setup

The restoration of noisy MR images has been analysed using synthetic MRI data sets from Brain Web and clinical data using the proposed adaptive hexagonal fuzzy bilateral filter. The quality of the MR image has been evaluated using PSNR, RMSE and SSIM.

The proposed adaptive hexagonal fuzzy bilateral filter and the existing methods are carried out using MATLAB 2013. The proposed adaptive hexagonal fuzzy bilateral filter has been compared with the existing techniques such as Median filter [24], NLM filter [27], Adaptive filter [12, 30, 33], Wiener filter [25], Bilateral filter [32], Fuzzy trapezoidal with NLM filter [35] and Fuzzy hexagonal with NLM filter [18].

4 Results and discussion

This section represents extensive experimental validation of the proposed adaptive hexagonal fuzzy bilateral filter using the synthetic MR image and clinical MR image as discussed in Section 3.1 and 3.2 respectively. The noise in MRI has been removed by restoration process using the proposed adaptive fuzzy hexagonal bilateral filter and its performance were compared with the existing methods such as Median filter, NLM filter, Adaptive filter, Bilateral filter, Wiener filter, Fuzzy trapezoidal with NLM filter and Fuzzy hexagonal with NLM filter. The efficiency of the proposed adaptive fuzzy hexagonal bilateral filter were analysed using the performance metrics PSNR, RMSE and SSIM.

4.1 Validation on synthetic MRI data

The synthetic MRI data with T1 weighed, T2 weighed and PD weighed were exploited at different noise levels. Table 1 shows the performance measures from low to high level noise for synthetic MRI image with T1 weighed, T2 weighed and PD weighed. The PSNR value obtained for the proposed adaptive fuzzy hexagonal bilateral filter is higher than the fuzzy hexagonal NLM filter. For higher rician noise level, NLM filter generates the artifacts on its own and fails to restore the noisy MRI accurately leads to the low PSNR value than the noisy image.

The bilateral filter in the proposed method has less computation cost than the NLM filter. Median filter preserves edges but fails to retain the structural information. Adaptive filter and wiener filter are unable to smooth the noise effectively. The NLM filter can able to preserve distinct edge features but it excessively smoothens the homogeneous regions and reduce the contrast between gray and white scale image [15] whereas the proposed adaptive fuzzy hexagonal bilateral filter preserves the edges and structural details of the image. Table 1 shows that mean of the proposed adaptive fuzzy hexagonal bilateral filter has 71, 72 and 72% for T1 weighted, T2 weighted and PD weighted respectively on average compared to fuzzy hexagonal NLM filter [5].

The differences in RMSE values of the proposed adaptive fuzzy hexagonal bilateral filter with the existing methods effectively characterize the performance of the restoration methods. Table 1, also shows the RMSE improvement of the processed image obtained by the proposed adaptive fuzzy hexagonal bilateral filter and existing filters. The proposed adaptive fuzzy hexagonal bilateral filter reduces RMSE by 99.6% for T1, 99.6% for T2 and 99.5% for PD compared to existing fuzzy hexagonal with NLM filter. SSIM quality index confirms the better visual quality of the proposed method at all noise levels. Figure 3 illustrates SSIM comparison of the proposed adaptive fuzzy hexagonal bilateral filter with other methods for the synthetic MRI. The proposed method gives much better SSIM improvement by retaining the structural details both at low and high level noise. The bilateral filter smoothen the local variations without affecting edges and the classification have been done using fuzzy hexagonal membership function improves the SSIM of noisy MRI both at low and high level.

Figure 4 shows the comparison of the synthetic MRI at 10% noise level. From the figure it is observed that the visual quality improvement achieved by the proposed adaptive fuzzy hexagonal bilateral filter reduces the noise and restore the original MRI effectively than existing methods. From the visual perception, it has been observed that the wiener filter is unable to smooth noise completely. NLM filter removes the noise but the structural information has been lost. When the noise level increases, the NLM filter with hexagonal MF and trapezoidal MF produced extra blur in the restoration. The proposed adaptive fuzzy hexagonal bilateral filter has the ability to reduce noise by retaining fine structural details and better edge preserving capabilties than existing methods.

4.2 Application to clinical MRI data

To evaluate the consistency of the proposed method on clinical MRI T1 weighted, T2 weighted and PD weighted images for varying rician noise ratio from 0.05 to 0.30 with a scale of 0.05 has been used. The quantitative metrics comparison for varying noise rates are tabulated in Tables 2 and 3. The proposed adaptive fuzzy hexagonal bilateral filter

Table 1 PSNR (RMSE) comparison on synthetic MR image at various noise level for the Median filter, NLM filter, Adaptive filter, Bilateral filter, Wiener filter, Fuzzy trapezoidal NLM filter, Fuzzy hexagonal NLM filter with the proposed adaptive Fuzzy hexagonal bilateral filter

Modality	Noise Level	Noisy Image	Median Filter	NLM Filter	Adaptive Filter	Bilateral Filter	Wiener Filter	Fuzzy Trapezoidal NLM filter	Fuzzy Hexagonal NLM filter	Proposed adaptive Fuzzy Hexagonal Bilateral filter
T1-weighted slice	0.05	24.67(10.56)	28.81(9.24)	27.05(11.33)	25.35(13.76)	68.82(0.09)	29.30(8.61)	28.65(9.42)	29.36(8.68)	75.39(0.036)
	0.10	22.76(16.69)	23.84(16.16)	20.67(23.61)	22.34(19.48)	67.11(0.11)	23.90(16.23	22.73(18.63)	24.95(16.28)	72.75(0.064)
	0.15	18.45(24.38)	20.03(25.10)	16.95(36.21)	19.31(27.62)	65.43(0.14)	19.80(26.83)	19.01(28.59)	20.10(25.19)	68.39(0.097)
	0.20	16.11(39.78)	17.07(34.51)	14.38(48.72)	16.77(36.99)	64.07(0.16)	16.88(36.48)	16.23(39.35)	17.18(35.29)	65.71(0.135)
	0.25	13.76(54.65)	14.18(44.39)	12.41(61.12)	14.76(46.63)	62.79(0.18)	14.72(46.76)	14.11(50.25)	14.95(45.60)	63.53(0.174)
	0.30	11.54(68.34)	13.03(54.69)	10.89(72.74)	13.12(56.29)	61.07(0.21)	13.05(56.72)	12.46(60.75)	13.26(55.40)	61.66(0.216)
	Mean	17.88(35.73)	19.49(30.68)	10.67(42.28)	18.61(33.46)	64.88(0.15)	19.61(31.94)	18.87(34.50)	19.97(31.07)	67.90(0.12)
T2-weighted slice	0.05	26.92(14.68)	27.55(10.68)	25.26(13.91)	26.35(12.27)	71.65(0.06)	28.27(9.83)	27.53(10.7)	27.85(10.32)	74.47(0.048)
	0.10	18.56(18.43)	22.48(19.16)	18.96(28.72)	21.15(22.33)	68.49(0.09)65	22.32(16.52)	21.83(20.65)	22.46(19.21)	69.54(0.085)
	0.15	14.74(28.48)	19.06(28.4)	15.47(42.96)	17.81(32.77)	65.90(0.13)	18.74(29.46)	18.28(31.07)	18.96(28.74)	66.30(0.12)
	0.20	13.35(45.43)	16.49(38.16)	12.99(57.11)	15.27(43.93)	64.07(0.16)	16.08(40)	15.65(48.06)	16.35(38.81)	63.67(0.167)
	0.25	11.96(64.78)	14.45(48.3)	11.11(70.96)	13.30(55.12)	60.67(0.22)	14.08(50.39)	13.62(53.14)	14.39(49.16)	61.68(0.21)
	0.30	09.32(70.21)	12.71(59.01)	9.56(84.76)	11.61(66.95)	57.59(0.24)	12.43(60.95)	11.9(64.77)	12.56(60.08)	59.97(0.255)
	Mean	15.80(40.34)	18.79(33.95)	15.56(49.74)	17.58(38.89)	64.73(0.15)	18.65(34.53)	18.14(38.07)	18.76(34.39)	65.94(0.147)
PD-weighted slice	0.05	25.12(10.52)	27.12(11.22)	25.62(13.35)	24.98(14.36)	68.94(0.09)	27.05(11.32)	27.39(10.88)	28.48(10.78)	73.88(0.05)
	0.10	21.36(17.63)	21.77(20.53)	19.32(27.95)	21.01(22.71)	67.13(0.11)	21.64(21.11)	21.55(21.34)	22.00(20.42)	69.65(0.084)
	0.15	17.67(34.89)	18.38(30.69)	15.76(41.53)	17.99(32.12)	65.15(0.14)	18.02(31.99)	17.90(32.41)	18.45(30.80)	66.50(0.12)
	0.20	14.35(42.56)	15.65(41.13)	13.28(55.27)	15.62(42.24)	63.50(0.17)	15.44(43.08)	15.25(44.05)	15.76(41.54)	64.15(0.16)
	0.25	11.34(56.67)	13.02(51.34)	11.38(68.78)	13.63(53.04)	61.32(0.21)	13.52(53.78)	13.25(55.47)	13.80(52.06)	62.14(0.19)
	0.30	09.86(65.21)	12.24(62.34)	9.88(81.76)	11.97(64.29)	60.36(0.24)	11.91(64.65)	11.56(67.39)	12.11(63.28)	60.55(0.24)
	Mean	16.61(37.91)	18.03(36.21)	15.87(48.11)	17.53(38.13)	64.40(0.16)	17.93(37.66)	17.82(38.59)	18.43(36.48)	66.15(0.14)
Overall Mean	–	16.76(37.99)	18.77(33.61)	14.03(46.71)	17.90(36.82)	64.67(0.15)	18.73(34.71)	18.27(37.05)	19.05(33.98)	66.66(0.14)

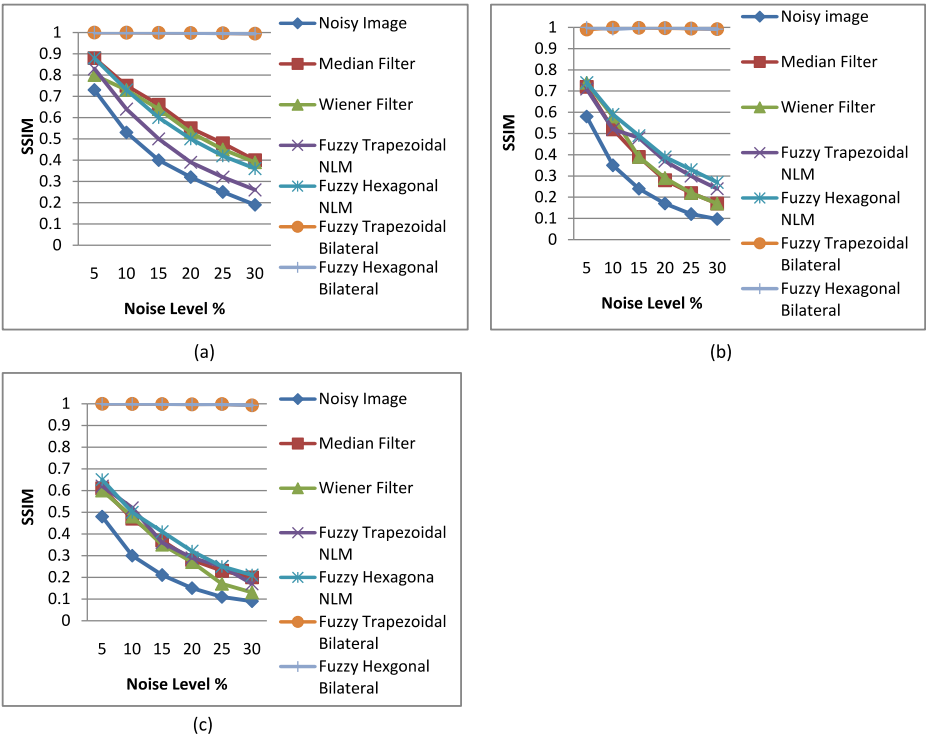

Fig. 3 SSIM comparsion for the synthetic MR data **a** T1 weighted **b** T2 weighted **c** PD weighted

restores the clinical MRI in both data sets better than existing methods, as it is easier to tune the decay of distance function in bilateral filtering. The edge preservation in the

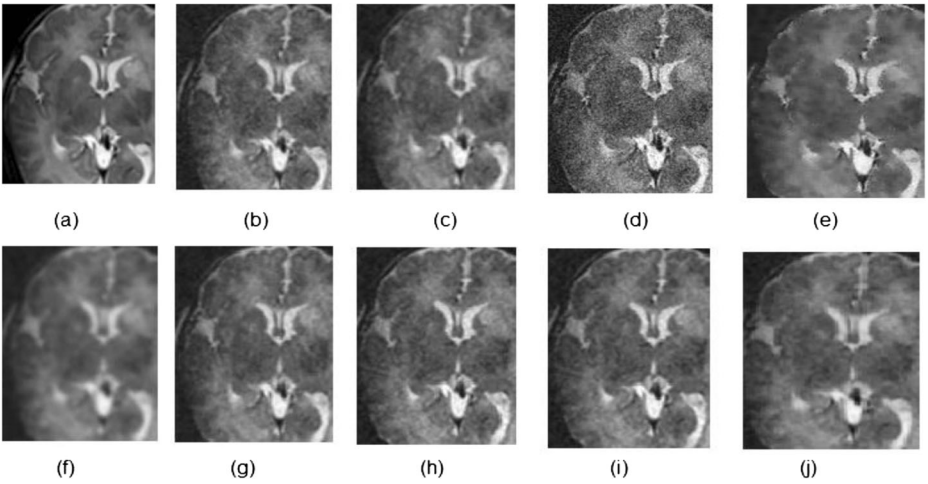

Fig. 4 Synthetic MRI with 10% noise **a** Original image **b** Rician noise image (PSNR = 22.76) **c** Median filter (PSNR = 23.84) **d** NLM filter (PSNR = 18.96) **e** Adaptive filter (PSNR = 21.15) **f** Bilateral filter (PSNR = 68.49) **g** Wiener filter (PSNR = 23.90) **h** Fuzzy trapezoidal MF with NLM filter (PSNR = 21.12) **i** Fuzzy hexagonal MF with NLM filter (PSNR = 21.42) **j** Proposed adaptive fuzzy hexagonal bilateral filter (PSNR = 69.94)

Table 2 PSNR (RMSE) comparison on clinical MR image at various noise level for the Median filter, NLM filter, Adaptive filter, Bilateral filter, Wiener filter, Fuzzy trapezoidal NLM filter, Fuzzy hexagonal NLM filter with the proposed adaptive Fuzzy hexagonal bilateral filter

Modality	Noise level	Noisy Image	Median Filter	NLM Filter	Adaptive Filter	Bilateral Filter	Wiener Filter	Fuzzy Trapezoidal NLM filter	Fuzzy Hexagonal NLM filter	Proposed adaptive Fuzzy Hexagonal Bilateral filter
T1-weighted slice	0.05	22.76(14.71)	27.03(11.35)	26.52(12.03)	27.14(11.19)	71.61(0.06)	28.21(9.56)	28.16(9.96)	29.23(9.9)	76.24(0.039)
	0.10	19.53(18.67)	24.85(14.59)	20.62(23.74)	25.79(13.08)	67.83(0.10)	25.56(13.44)	23.72(16.63)	25.18(14.04)	75.19(0.044)
	0.15	16.35(27.86)	22.32(19.08)	17.39(34.40)	23.72(16.62)	65.03(0.14)	22.18(18.51)	20.56(23.93)	22.46(19.29)	72.44(0.050)
	0.20	13.42(34.67)	19.19(25.94)	15.11(44.76)	21.44(21.60)	63.06(0.18)	19.23(25.83)	18.10(31.73)	19.95(25.65)	70.15(0.079)
	0.25	10.75(46.87)	16.90(33.12)	13.40(54.51)	19.26(27.76)	61.76(0.21)	17.05(33.91)	16.09(39.95)	17.77(32.95)	69.89(0.07)
	0.30	09.67(55.38)	15.21(39.46)	12.07(63.50)	17.25(34.96)	60.98(0.23)	15.29(39.05)	14.47(48.18)	15.99(40.45)	66.93(0.13)
	Mean	15.42(33.03)	20.92(23.92)	17.51(38.82)	22.43(20.86)	65.05(0.15)	21.25(23.38)	20.18(28.40)	21.76(23.71)	71.81(0.07)
T2-weighted slice	0.05	25.32(16.89)	26.01(12.76)	24.93(14.45)	26.87(11.55)	70.62(0.07)	26.34(11.94)	27.01(11.31)	28.18(11.14)	80.77(0.023)
	0.10	21.25(19.53)	24.79(14.67)	20.46(24.16)	25.98(12.79)	67.75(0.10)	24.89(13.99)	23.88(16.3)	25.23(13.46)	75.51(0.042)
	0.15	17.67(26.45)	22.41(19.30)	17.04(35.85)	24.04(16.01)	64.95(0.14)	22.65(18.78)	20.61(23.77)	23.85(19.44)	71.99(0.060)
	0.20	15.67(37.58)	19.09(25.22)	14.65(47.19)	21.79(20.75)	63.7(0.18)	19.3(24.59)	17.8(32.56)	19.82(26.03)	68.13(0.10)
	0.25	11.48(43.56)	17.76(32.25)	13.02(56.91)	19.56(26.81)	61.74(0.21)	18.14(31.57)	16.00(40.40)	18.68(33.29)	66.62(0.13)
	0.30	08.78(58.97)	16.15(39.74)	11.67(66.48)	17.51(33.97)	60.94(0.23)	16.45(38.39)	14.29(49.17)	16.89(41.03)	63.55(0.18)
	Mean	16.69(33.83)	21.04(23.99)	16.96(40.84)	22.63(20.31)	64.95(0.16)	21.30(23.21)	19.93(28.92)	22.11(24.07)	71.10(0.09)
PD-weighted slice	0.05	23.64(15.37)	26.08(11.64)	25.4(13.63)	24.34(15.46)	69.95(0.08)	26.07(11.65)	26.68(11.81)	27.95(11.32)	74.10(0.050)
	0.10	20.70(19.54)	21.05(21.43)	19.12(28.12)	20.62(23.76)	67.69(0.11)	21.25(22.06)	20.81(23.22)	21.46(21.55)	69.65(0.083)
	0.15	17.78(26.77)	18.01(31.43)	15.61(42.26)	17.67(33.34)	65.55(0.13)	17.80(32.83)	17.38(34.47)	18.70(31.83)	66.35(0.122)
	0.20	14.52(31.63)	15.58(41.41)	13.23(55.56)	15.43(43.17)	62.89(0.17)	15.36(43.49)	14.9(45.59)	16.64(42.11)	63.98(0.162)
	0.25	11.42(38.67)	13.24(52.40)	11.34(69.06)	13.53(53.67)	61.62(0.21)	13.42(54.35)	12.96(57.26)	13.61(53.22)	63.04(0.20)
	0.30	09.13(48.94)	12.11(63.28)	9.98(80.80)	12.67(63.52)	59.68(0.27)	11.83(65.28)	11.36(68.90)	12.00(64.23)	60.42(0.25)
	Mean	16.19(30.15)	17.68(36.93)	15.78(36.73)	17.38(38.82)	64.56(0.16)	17.62(38.28)	17.35(40.21)	18.39(37.38)	66.26(0.14)
Overall Mean	–	16.1(32.34)	19.88(28.28)	16.75(38.79)	20.81(26.66)	64.85(0.16)	20.06(28.29)	19.15(32.51)	20.75(28.39)	69.72(0.1)

Table 3 PSNR (RMSE) comparison on clinical MR image for public dataset at various noise level for the Median filter, NLM filter, Adaptive filter, bilateral filter, Wiener filter, Fuzzy trapezoidal NLM filter, Fuzzy hexagonal NLM filter with the proposed adaptive Fuzzy hexagonal bilateral filter

Modality	Noise level	Noisy Image	Median Filter	NLM Filter	Adaptive Filter	Bilateral Filter	Wiener Filter	Fuzzy Trapezoidal NLM filter	Fuzzy Hexagonal NLM filter	Proposed adaptive Fuzzy Hexagonal Bilateral filter
T1-weighted slice	0.05	24.36(0.067)	31.00(11.71)	27.05(11.33)	28.78(9.27)	73.28(0.07)	34.10(9.06)	25.18(15.75)	26.22(15.6)	75.49(0.067)
	0.10	21.45(0.15)	29.6(22.04)	20.54(23.95)	24.52(15.14)	70.52(0.08)	30.04(18.66)	21.59(21.22)	22.15(19.88)	72.17(0.072)
	0.15	18.05(0.146)	27.00(34.11)	16.96(36.14)	20.76(23.34)	68.13(0.09)	26.72(32.12)	18.62(21.87)	19.58(26.76)	69.02(0.08)
	0.20	15.72(0.2)	25.50(41.14)	14.55(47.75)	18.15(31.55)	65.98(0.13)	26.07(43.13)	16.32(38.95)	17.35(34.58)	66.38(0.12)
	0.25	10.65(0.27)	23.60(53.18)	12.65(59.39)	16.04(40.19)	64.04(0.16)	23.71(56.77)	14.35(48.81)	15.43(43.55)	65.52(0.15)
	0.30	09.25(0.32)	22.02(69.20)	11.22(70.03)	14.35(48.87)	62.39(0.19)	21.99(70.20)	12.79(58.45)	13.73(52.50)	63.49(0.19)
	Mean	16.58(0.192)	26.45(38.56)	17.16(41.47)	20.43(28.06)	67.39(0.12)	27.11(38.32)	18.14(34.18)	19.08(32.15)	68.68(0.11)
T2-weighted slice	0.05	26.57(0.09)	33.53(11.05)	24.89(14.51)	24.83(14.61)	68.55(0.09)	33.75(11.05)	25.86(12.97)	25.75(13.15)	74.72(0.04)
	0.10	22.29(0.12)	27.92(23.10)	18.43(30.55)	18.43(26.35)	65.82(0.13)	27.78(23.1)	19.76(26.20)	19.94(25.67)	68.15(0.08)
	0.15	16.81(0.156)	24.55(32.15)	14.79(46.41)	14.79(39.38)	63.40(0.17)	24.27(32.55)	16.13(39.79)	16.38(38.71)	65.56(0.14)
	0.20	14.28(0.23)	22.02(44.20)	12.29(61.9)	12.29(52.46)	61.34(0.21)	21.69(41.20)	13.56(53.50)	13.83(51.83)	62.72(0.19)
	0.25	13.36(0.32)	20.00(55.25)	10.35(77.41)	10.35(65.27)	59.55(0.27)	19.65(53.6)	11.59(67.18)	11.89(64.97)	60.85(0.24)
	0.30	11.86(0.38)	18.40(72.30)	8.87(91.83)	8.87(78.84)	58.12(0.32)	18.09(69.31)	9.98(80.75)	10.29(77.94)	58.66(0.29)
	Mean	17.53(0.22)	24.40(39.66)	14.94(53.77)	14.93(46.15)	62.80(0.2)	24.21(38.47)	16.15(46.73)	16.35(45.38)	65.11(0.16)
PD-weighted slice	0.05	24.41(0.06)	36.2(10.03)	27.08(11.28)	31.11(7.09)	72.54(0.06)	38.58(10.04)	29.96(8.09)	31.28(6.96)	79.50(0.02)
	0.10	18.12(0.1)	33.21(20.05)	20.43(24.27)	25.15(13.15)	70.78(0.07)	33.38(21.54)	23.23(17.57)	24.88(14.53)	73.78(0.05)
	0.15	14.56(0.19)	29.26(30.08)	16.73(37.16)	21.1(20.69)	68.51(0.09)	29.05(34.08)	19.29(27.64)	20.83(23.18)	69.70(0.08)
	0.20	12.17(0.28)	26.52(44.12)	14.28(49.24)	18.86(29.07)	66.46(0.12)	26.25(42.12)	16.66(37.45)	18.09(31.76)	67.03(0.11)
	0.25	10.50(0.32)	24.35(58.15)	12.48(60.62)	16.77(36.97)	64.66(0.15)	24.22(50.16)	14.61(47.38)	15.89(40.90)	64.89(0.14)
	0.30	09.20(0.38)	22.53(67.19)	11.20(70.22)	15.08(44.92)	63.05(0.18)	22.57(68.19)	13.09(57.46)	14.19(49.72)	63.90(0.17)
	Mean	14.82(0.22)	28.68(38.27)	17.03(42.13)	21.35(25.32)	67.67(0.11)	29.01(37.69)	19.47(32.59)	20.86(27.84)	69.80(0.18)
Overall Mean	–	64.75(0.21)	26.51(38.83)	16.38(45.79)	18.90(33.18)	65.95(0.14)	26.78(38.16)	17.92(37.83)	18.76(35.12)	67.86(0.15)

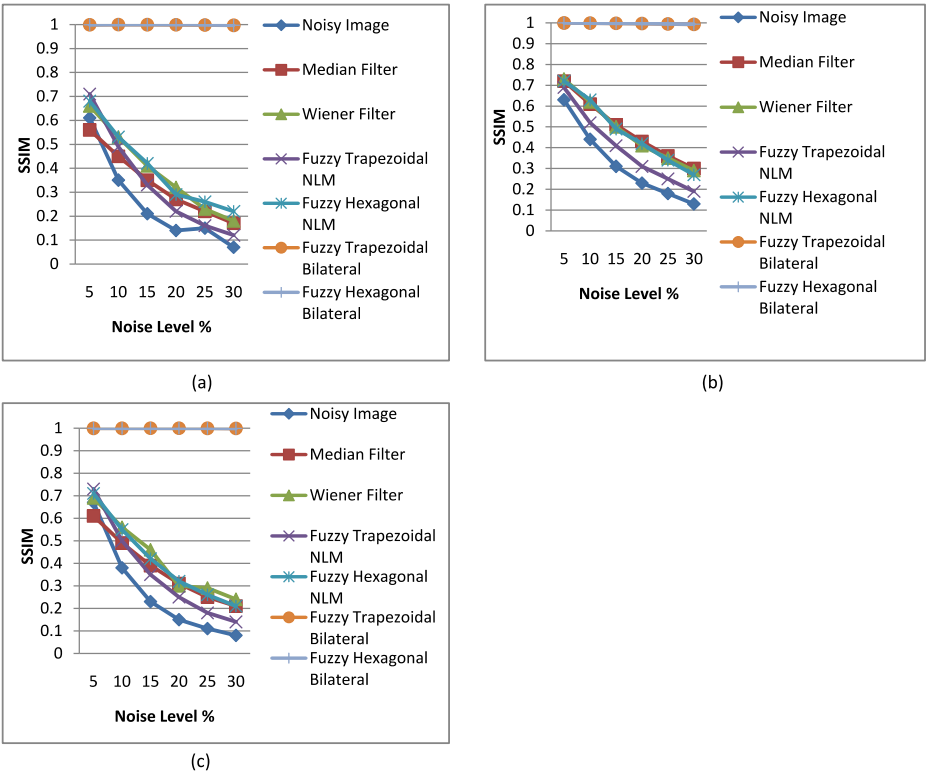

Fig. 5 SSIM comparison for the clinical MRI **a** T1 weighted **b** T2 weighted **c** PD weighted

proposed method is higher, as it averages within smooth regions of the image than averaging across image edges are shown in Tables 2 and 3 respectively.

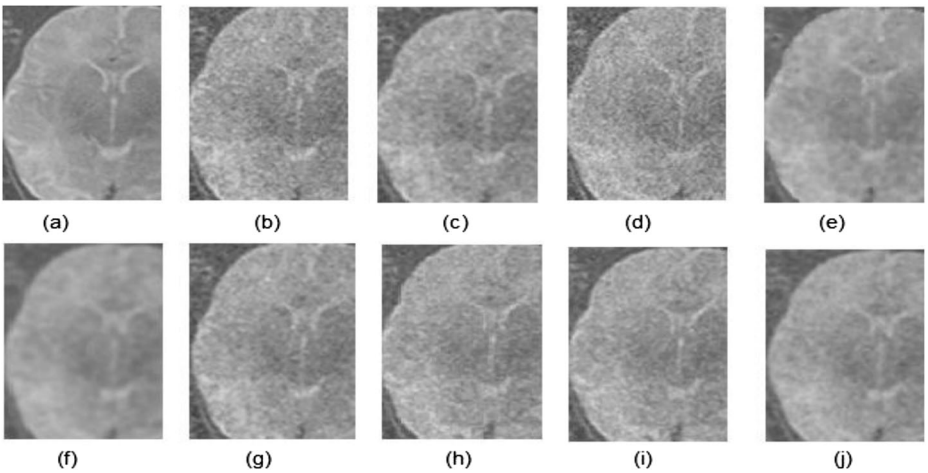

Fig. 6 Clinical MRI with 10% noise **a** Original image **b** Rician noise image (PSNR = 19.53) **c** Median filter (PSNR = 24.85) **d** NLM filter (PSNR = 20.46) **e** Adaptive filter (PSNR = 25.98) **f** Bilateral filter (PSNR = 67.75) **g** Wiener filter (PSNR = 25.56) **h** Fuzzy trapezoidal MF with NLM filter (PSNR = 23.45) **i** Fuzzy hexagonal MF with NLM filter (PSNR = 25.68) **j** Proposed adaptive fuzzy hexagonal bilateral filter (PSNR = 75.29)

The proposed adaptive fuzzy hexagonal bilateral filter has been quantitatively compared with existing methods, to analyze the SSIM for all noise levels for clinical dataset as shown in Fig. 5. The qualitatively analysis is shown for the clinical dataset in Fig. 6 and from the Fig. 6 it gives residue significantly less compared to other methods. In Figs. 6 and 7 the clinical public dataset are analysed and it result shows high performance for the proposed method. The proposed method shows better edge preserving potential due to adaptive weight adjustment compared to existing methods.

The enhanced accuracy of the proposed adaptive hexagonal bilateral filter can be understood by considering the two facts; First, fuzzy classification has been done adaptively using hexagonal membership function. Second, the implementation to classifying the pixel with additional scalar parameters to tune the proposed method effectively than the trapezoidal membership functions. Although the parameter is more but the effectiveness of the restoration obtained by proposed adaptive fuzzy hexagonal bilateral filter method makes reliable. The restored MRI image is noiseless due to the adaptive nature of noisy image in hexagonal fuzzy membership function.

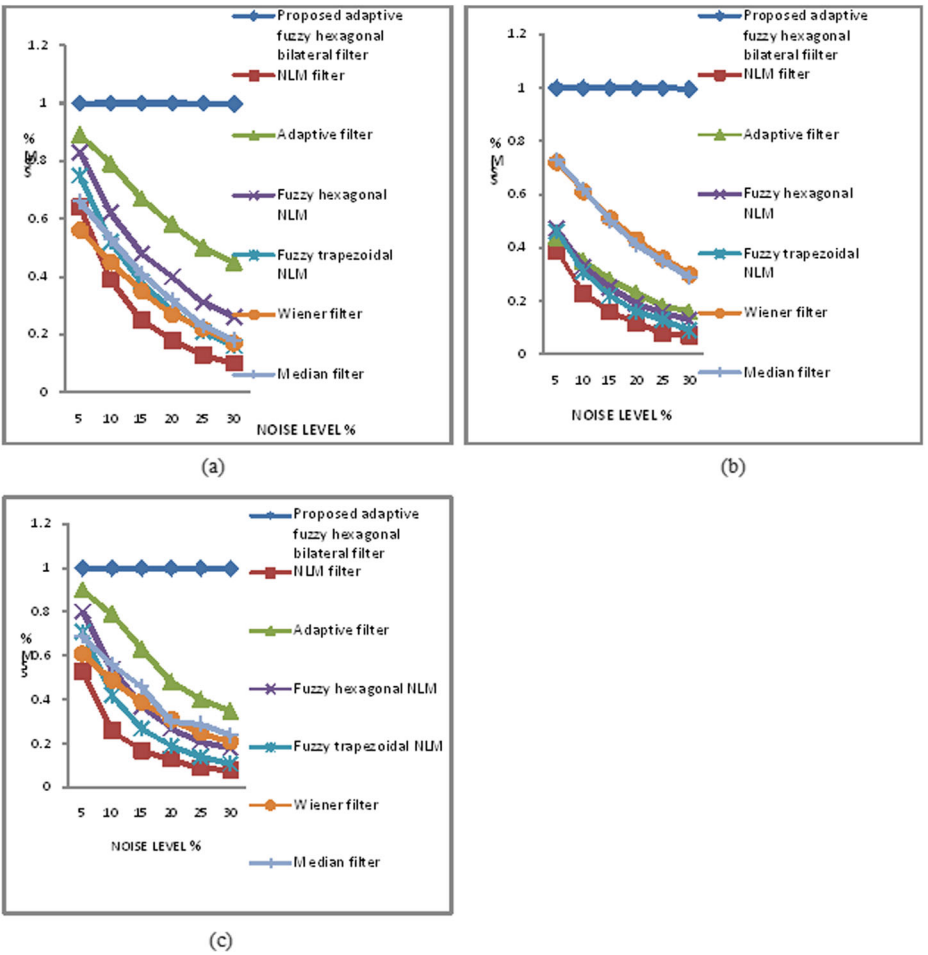

Fig. 7 SSIM comparison for the clinical MRI for public dataset **a** T1 weighted **b** T2 weighted **c** PD weighted

5 Conclusion

In this paper, adaptive fuzzy hexagonal bilateral filter has been presented and analyzed for Brain MRI denoising application. This method increases the PSNR without affecting the significant structures in the image. Although RMSE is a quantitative parameter, the visual perception sense and SSIM guarantee have been analysed. The visual inspection of the proposed method based on image residuals evaluates the efficiency. In future, the estimation of the noise level will be determined before restoration process and then analysis the restored MRI.

Acknowledgments The authors are grateful for the financial support provided by University Grants Commission (UGC) under Rajiv Gandhi National Fellowship, New Delhi, India. Grant number: F1-17.1/2016-17/RGNF-2015-17-SC-TAM-23661.

Compliance with ethical standards

Conflict of interest There is no conflict of interest.

References

1. Abazari R, Lakestani M (2017) Fourier based discrete Shearlet transform for speckle noise reduction in medical ultrasound images. Current Medical Imaging. https://doi.org/10.2174/1573405613666170405150822
2. Abazari R, Lakestani M (2018) A hybrid denoising algorithm based on shearlet transform method and Yaroslavsky's filter. Multimed Tools Appl. https://doi.org/10.1007/s11042-018-5648-7
3. Akar SA (2016) Determination of optimal parameters for bilateral filter in brain MR image denoising. Appl Soft Comput 43:87–96
4. Alhihi M, Khosravi MR (2018) Operating task redistribution in hyperconverged networks. International Journal of Electrical and Computer Engineering 8(3):1629–1635
5. Alhihi M, Khosravi MR (2018) Formulizing the fuzzy rule for Takagi-Sugeno approach in network traffic control. The Open Electrical & Electronic Engineering Journal 12(1):1–11
6. Alhihi M, Khosravi MR, Attar H, Samou M (2017) Determining the optimum number of paths for realization of multi-path routing in MPLS-TE networks. TELKOMNIKA 15(4):1701–1709
7. Anand CS, Sahambi JS (2010) Wavelet domain non-linear filtering for MRI denoising. Magn Reson Imaging 28:842–861
8. Ashburner J, Friston K (2000) Voxel-based morphometry – the methods. NeuroImage 11:805–821
9. Chen Y, Yang J, Zhang Y, Shu H et al (2016) Structure-adaptive fuzzy estimation for random-valued impulse noise suppression. IEEE Trans Circuits Syst Video Technol. https://doi.org/10.1109/TCSVT.2016.2615444
10. Dougherty G (2009) Digital image processing for medical applications. Cambridge University Press, Cambridge
11. Edelstein WA, Glover GH, Hardy CJ, Redington RW (1986) The intrinsic SNR in NMR imaging. Magn Reson Med 3(4):604–618
12. Gerig G, Kubler O, Kikinis R, Jolesz FA (1992) Nonlinear anisotropic filtering of MRI data. IEEE Trans Med Imaging 11(2):221–232
13. Henkelman RM (1985) Measurement of signal intensities in the presence of noise in mr images. Med Phys 12(2):232–233
14. http://www.insight-journal.org/midas/. Accessed 01 July 2017
15. Hu J, Zhou J, Wu X (2016) Non-local MRI denoising using random sampling. Magn Reson Imaging 34:990–999
16. Isik A, Firat D (2017) Bilateral intra-areolar polythelia. Breast J. https://doi.org/10.1111/tbj.12838
17. Justin J, Sivaraman J, Rajadurai P, Simiv R (2017) An edge preservation index for evaluating nonlinear spatial restoration in MR images. Current Medical Imaging 13(1):58–65
18. Kala R, Deepa P (2017) Adaptive hexagonal fuzzy hybrid filter for Rician noise removal in MRI images. Neural Comput & Applic 29(8):237–249
19. Kaur P, Singh G, Kaur P (2017) A review of Denoising medical images using machine learning approaches. Current Medical Imaging. https://doi.org/10.2174/1573405613666170428154156

20. Khan SU, Ullah N, Ahmed I, Chai WY, Khan A (2017) MRI images enhancement using genetic programming based hybrid noise removal filter approach. Current Medical Imaging. https://doi.org/10.2174/1573405613666170619093021
21. Khosravi MR, Akbarzadeh O, Salari SR, Samadi S, Rostami H (2017) An introduction to ENVI tools for synthetic aperture radar (SAR) image despeckling and quantitative comparison of denoising filters. In: IEEE international conference on power, control, signals and instrumentation engineering (ICPCSI), India
22. Khosravi MR, Basri H, Rostami H (2018) Efficient routing for dense UWSNs with high-speed Mobile nodes using spherical divisions. J Supercomput 74(2):696–716
23. Kumarganesh S, Suganthi M (2018) An enhanced medical diagnosis sustainable system for brain tumor detection and segmentation using ANFIS classifier. Current Medical Imaging 14(2):271–279
24. Lim JS (1990) Two-dimensional signal and image processing. Prentice Hall, Englewood Cliffs, pp 469–476
25. Lim JS (1990) Two-dimensional signal and image processing. Prentice Hall, Englewood Cliffs, p 548
26. Lujan HJ, Plasencia G, Rivera BX et al (2017) Advantages of robotic right colectomy with Intracorporeal anastomosis. Surg Laparosc Endosc Percutan Tech 28(1):36–41. https://doi.org/10.1097/sle.0000000000000384
27. Manjon JV, Carbonell-Caballero J, Lull JJ, Garcia-Marti G, Marti-Bonmati L, Robles M (2008) MRI denoising using non-local means. Med Image Anal 12:514–523
28. Misra D, Sarker S, Dhabal S, Ganguly A (2013) Effect of using genetic algorithm to de-noise MRI images corrupted with Rician noise. In: IEEE international conference on emerging trends in computing, communication and nanotechnology, Tirunelveli, India, pp 146–151
29. Nowak RD (1999) Wavelet-based Rician noise removal for magnetic resonance imaging. IEEE Trans Image Process 8(10):1408–1419
30. Perona P, Malik J (1990) Scale-space and edge detection using anisotropic diffusion. IEEE Trans Pattern Anal Mach Intell 12:629–639
31. Phophalia A, Mitra SK (2015) Rough set based bilateral filter design for denoising brain MR images. Appl Soft Comput. https://doi.org/10.1016/j.asoc.2015.04.005
32. Riji R, Jeny R, Jan S, Madhu NS (2015) Iterative bilateral filter for Rician noise reduction in MR images. Signal, Image and Video Processing 9(7):1543–1548
33. Samsonov AA, Johnson CR (2004) Noise-adaptive nonlinear diffusion filtering of MR images with spatially varying noise levels. Magn Reson Med 52:798–806
34. Sharif M, Hussain A, Jaffar MA, Choi T-S (2015) Fuzzy similarity based non local means filter for rician noise removal. Multimed Tools Appl 74(15):5533–5556
35. Sharif M, Hussain A, Jaffar MA, Choi T-S (2016) Fuzzy-based hybrid filter for rician noise removal. SIViP 10(2):215–224
36. Sudeep PV, Palanisamy P, Chandrasekharan K, Jeny R (2015) Nonlocal linear minimum mean square error methods for denoising MRI. Biomed Signal Process Control 20:125–134
37. Yingtao Z, Cheng HD, Huang J, Tang X (2012) An effective and objective criterion for evaluating the performance of denoising filters. Pattern Recogn 45:2743–2757
38. Zhang Y-D, Pan C, Sun J, Tang C (2018) Multiple sclerosis identification by convolutional neural network with drop out and parametric ReLU. J Comput Sci. https://doi.org/10.1016/j.jocs.2018.07.03

Kala R received the Bachelor Degree in Electrical and Electronics Engineering in 2004 from Manonmaniam Sundaranar University, Tirunelveli, Tamilnadu, India. She received the M.E. degree in Computer Science and Engineering in the year 2007. She had 5 years of teaching experience and currently pursuing full time research in the Department of Electronics and Communication Engineering, Government College of Technology, Coimbatore, Tamil Nadu, India. The research area includes Image Processing, Neural Networks and Data Structures.

Deepa P received the Bachelor Degree in Electronics and Communication Engineering in 2002 from Bharathiyar University, Coimbatore, Tamil Nadu, India. She received M.E. degree in VLSI Design in the year 2007 and Ph.D. degree in Information and Communication Engineering in 2013 from Anna University, Chennai, Tamil Nadu, India. She is working as an Assistant Professor, Department of Electronics and Communication Engineering, Government College of Technology, Coimbatore, Tamil Nadu, India. Her research area includes Low Power VLSI Design and Image Processing. Her research papers published in various journals and she presented papers in national and international conferences.